

## LETTER TO THE EDITOR

# AP4 induces JNK1 and a miR-22-3p/*FOSL1* feed-forward loop to activate AP-1 and promote colorectal cancer metastasis

Dear Editor,

Colorectal cancer (CRC) is the third most deadly cancer worldwide [1]. The mortality of CRC has remained high due to limited treatment options for metastatic CRC (mCRC) [2]. Epithelial-mesenchymal transition (EMT) is an important contributor to mCRC [2]. The c-MYC proto-oncogene (MYC)-induced transcription factor AP4 (TFAP4/AP4) is a driver of EMT, thereby presumably facilitates mCRC [3, 4]. The mitogen-activated protein kinase (MAPK)/c-Jun N-terminal kinase (JNK)/activator protein-1 (AP-1) pathway has been implicated in the regulation of EMT and mCRC [5].

Here, we analyzed whether AP4 regulates components of the MAPK/JNK/AP-1 pathway after MYC activation using CRC cells rendered AP4-deficient by a clustered regularly interspaced short palindromic repeats (CRISPR)/CRISPR-associated protein 9 (Cas9) approach. The detailed methods are shown in the Supplementary file. First, we grouped MYC-induced changes in mRNA expression observed in the CRC cell line DLD-1 AP4 wild-type 1/pRTR-c-MYC-VSV (AP4-WT1 DLD-1/pRTR-c-

MYC-VSV) into 6 non-overlapping expression clusters (Supplementary Figure S1A, left), with cluster 1 representing mRNAs down-regulated, and clusters 2-6 representing different patterns of mRNA up-regulated after MYC activation. MAPK signaling pathway components were strongly over-represented in cluster 6 (Supplementary Figure S1A, right). The AP4 targets *MIR22 host gene* (*MIR22HG*) and *E-cadherin 1* (*CDH1*) were down-regulated after MYC activation in AP4-WT1 DLD-1/pRTR-c-MYC-VSV cells (Supplementary Figure S1B). MAPK signaling effectors, including *c-Fos proto-oncogene* (*FOS*), *c-Jun proto-oncogene* (*JUN*) and *c-JunB proto-oncogene* (*JUNB*), were over-represented in cluster 6. Additional MAPK signaling pathway components, such as *c-Jun N-terminal kinase 1* (*JNK1*), *mitogen-activated protein kinase kinase 1* (*MAP3K1*), *mitogen-activated protein kinase kinase 13* (*MAP3K13*), *mitogen-activated protein kinase kinase 3* (*MAP2K3*), *mitogen-activated protein kinase kinase 7* (*MAP2K7*) and *FOS-like 1* (*FOSL1*) were found in clusters 3-5 (Supplementary Figure S1B). Interestingly, *MAP3K13*, *MAP2K7*, *JNK1* and *FOSL1* were induced by MYC in an AP4-dependent manner (Supplementary Figure S1C-D).

Notably, *MAP3K13*, *FOSL1*, *JNK1* and *MAP2K7* were also up-regulated after activating AP4 for 48 or 72 hours (Figure 1A) and showed AP4-binding sites (CAGCTG) and AP4 occupancy (Supplementary Figure S2A). Therefore, these genes presumably represent direct AP4 targets. *MAP3K13* and *FOSL1* protein and phosphorylated *JNK1* were up-regulated after AP4 activation, whereas *JNK1* protein levels remained unchanged (Figure 1B). Furthermore, AP4 occupancy at the *MAP3K13* and *FOSL1* promoters was confirmed by quantitative real-time polymerase chain reaction-chromatin immunoprecipitation (qChIP) analysis (Figure 1C). The nascent mRNA of *MAP3K13* and *FOSL1* was decreased in AP4-deficient DLD-1 and SW480 cells (Supplementary Figure S2B). Ectopic AP4 induced nascent *MAP3K13* and *FOSL1* mRNA in CRC cells (Supplementary Figure S2C). Therefore, AP4 activates the *JNK1* pathway through a *MAP3K13*/*MAP2K7*/*JNK1* cascade. CRCs with liver metastasis are significantly more

**List of Abbreviations:** 3'-UTR, 3'-untranslated region; AP-1, activator protein-1; Cas9, clustered regularly interspaced short palindromic repeats-associated protein 9; *CDH1*, E-cadherin 1; *MYC*, c-MYC proto-oncogene; CRC, colorectal cancer; CRISPR, clustered regularly interspaced short palindromic repeats; DOX, doxycycline; EMT, epithelial-mesenchymal transition; *FOSL1*/*FRA1*, FOS-like 1/*FOS*-related antigen 1; *JNK1*, c-Jun N-terminal protein kinase 1; *JUN*, *c-Jun* proto-oncogene; *JUNB*, *c-JunB* proto-oncogene; KO, knock-out; *MAP2K7*, mitogen-activated protein kinase kinase 7; *MAP3K13*, mitogen-activated protein kinase kinase 13; MAPK, mitogen-activated protein kinase; mCRC, metastatic colorectal cancer; *MDC1*, mediator of DNA damage checkpoint 1; *MIR22HG*, *MIR22* host gene; MUT, mutant; NOD/SCID, non-obese diabetic/severe combined immunodeficiency; qChIP, quantitative real-time polymerase chain reaction-chromatin immunoprecipitation; qPCR, quantitative real-time polymerase chain reaction; SMS, seed-matching sequence;  $t_{1/2}$ , half-life time; TCGA-COAD, The Cancer Genome Atlas Colorectal Adenocarcinoma; TF, transcription factor; TFAP4/AP4, transcription factor AP4/activating enhancer binding protein 4; VIM, vimentin; WT, wild-type;  $\Delta$ SMS, seed-matching sequence deletion.

This is an open access article under the terms of the [Creative Commons Attribution-NonCommercial-NoDerivs](https://creativecommons.org/licenses/by-nc-nd/4.0/) License, which permits use and distribution in any medium, provided the original work is properly cited, the use is non-commercial and no modifications or adaptations are made.

© 2024 The Authors. *Cancer Communications* published by John Wiley & Sons Australia, Ltd. on behalf of Sun Yat-sen University Cancer Center.

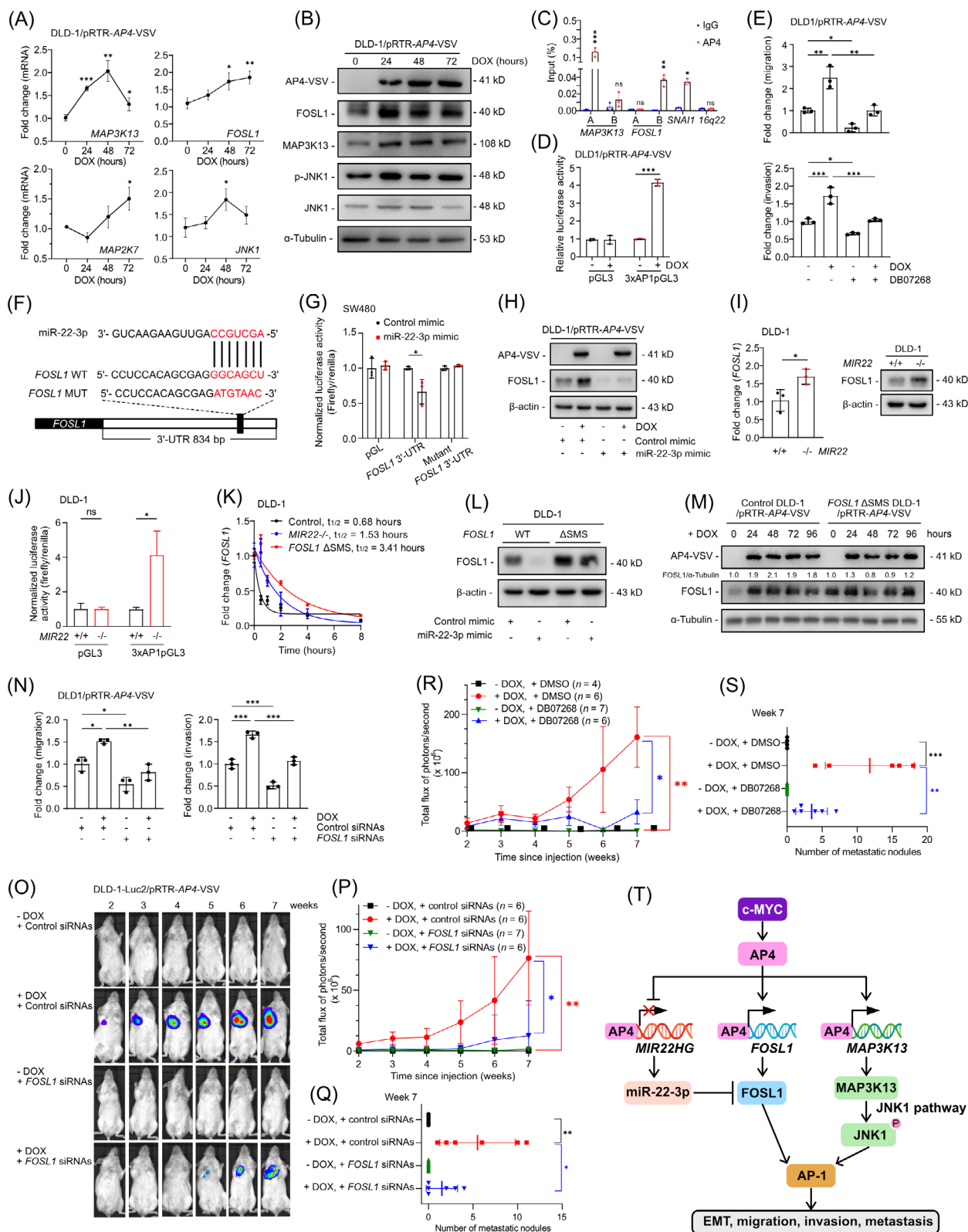


**FIGURE 1** AP4 induces JNK1 and a miR-22-3p/FOSL1 feed-forward loop to activate AP-1 and promote colorectal cancer metastasis. (A) DLD-1/pRTR-AP4-VSV cells were treated with DOX to induce AP4 expression for 0, 24, 48 and 72 hours. The mRNA expression of *MAP3K13*, *FOSL1*, *MAP2K7* and *JNK1* was analyzed by qPCR. Expression was normalized to *GAPDH* and untreated controls (0 hours DOX). (B) Western blot analysis of FOSL1, MAP3K13 and JNK1 in DLD-1/pRTR-AP4-VSV cells after treatment with DOX to induce AP4 expression for 0, 24, 48 and 72 hours.  $\alpha$ -Tubulin served as a loading control. (C) Validation of *MAP3K13* and *FOSL1* as direct targets of AP4 via qChIP assay. The predicted E-boxes (CAGCTG) in *MAP3K13* and *FOSL1* were analysed. DLD-1/pRTR-AP4-VSV cells were treated with DOX for 48 hours or left untreated before immunoprecipitation with anti-AP4 or anti-rabbit-IgG antibodies. *SNAIL1* and *16q22* served as positive and negative controls, (D) DLD-1/pRTR-AP4-VSV cells treated with DOX (0, 24, 48, 72 hours). Relative luciferase activity of *MAP3K13* and *FOSL1* reporter constructs analyzed by luciferase assay. pGL3 and 3xAP1pGL3 served as positive and negative controls. (E) DLD-1/pRTR-AP4-VSV cells treated with DOX (0, 24, 48, 72 hours). Fold change (migration) and fold change (invasion) analyzed by Transwell assay. DB07268 served as a positive control. (F) miR-22-3p 3'-GUCAAGAAGUUGACCGUCGA-5' and FOSL1 WT 5'-CCUCCACAGCGAGGGCAGCU-3' and FOSL1 MUT 5'-CCUCCACAGCGAGATGTAAC-3' sequences. FOSL1 3'-UTR 834 bp. (G) SW480 cells treated with Control mimic or miR-22-3p mimic. Normalized luciferase activity (Firefly/renilla) analyzed by luciferase assay. pGL, FOSL1 3'-UTR, and FOSL1 3'-UTR mutant served as positive and negative controls. (H) DLD-1/pRTR-AP4-VSV cells treated with DOX (0, 24, 48, 72 hours). Western blot analysis of FOSL1 and  $\beta$ -actin. Control mimic and miR-22-3p mimic served as positive and negative controls. (I) DLD-1 cells treated with Control mimic or miR-22-3p mimic. Fold change (FOSL1) analyzed by luciferase assay. MIR22 +/+ and -/- served as positive and negative controls. (J) DLD-1 cells treated with Control mimic or miR-22-3p mimic. Normalized luciferase activity (Firefly/renilla) analyzed by luciferase assay. pGL3 and 3xAP1pGL3 served as positive and negative controls. (K) DLD-1 cells treated with Control mimic or miR-22-3p mimic. Fold change (FOSL1) analyzed by luciferase assay. Control mimic, t<sub>1/2</sub> = 0.68 hours; miR-22-3p mimic, t<sub>1/2</sub> = 1.53 hours; FOSL1  $\Delta$ SMS, t<sub>1/2</sub> = 3.41 hours. (L) DLD-1 cells treated with Control mimic or miR-22-3p mimic. Western blot analysis of FOSL1 and  $\beta$ -actin. Control mimic and miR-22-3p mimic served as positive and negative controls. (M) Control DLD-1/pRTR-AP4-VSV and FOSL1  $\Delta$ SMS DLD-1/pRTR-AP4-VSV cells treated with DOX (0, 24, 48, 72, 96 hours). Western blot analysis of AP4-VSV, FOSL1/ $\alpha$ -Tubulin, and  $\alpha$ -Tubulin. FOSL1 and  $\alpha$ -Tubulin served as positive and negative controls. (N) DLD-1/pRTR-AP4-VSV cells treated with DOX (0, 24, 48, 72 hours). Fold change (migration) and fold change (invasion) analyzed by Transwell assay. Control siRNAs and FOSL1 siRNAs served as positive and negative controls. (O) DLD-1-Luc2/pRTR-AP4-VSV cells treated with DOX (0, 24, 48, 72 hours). Bioluminescence images of mice treated with DOX and Control siRNAs, DOX and FOSL1 siRNAs, or DOX and FOSL1 siRNAs. (P) DLD-1-Luc2/pRTR-AP4-VSV cells treated with DOX (0, 24, 48, 72 hours). Total flux of photons/second (x 10<sup>6</sup>) analyzed by bioluminescence assay. Control siRNAs and FOSL1 siRNAs served as positive and negative controls. (Q) DLD-1-Luc2/pRTR-AP4-VSV cells treated with DOX (0, 24, 48, 72 hours). Number of metastatic nodules analyzed by bioluminescence assay. Control siRNAs and FOSL1 siRNAs served as positive and negative controls. (R) DLD-1-Luc2/pRTR-AP4-VSV cells treated with DOX (0, 24, 48, 72 hours). Total flux of photons/second (x 10<sup>6</sup>) analyzed by bioluminescence assay. Control siRNAs and FOSL1 siRNAs served as positive and negative controls. (S) DLD-1-Luc2/pRTR-AP4-VSV cells treated with DOX (0, 24, 48, 72 hours). Number of metastatic nodules analyzed by bioluminescence assay. Control siRNAs and FOSL1 siRNAs served as positive and negative controls. (T) Schematic diagram of the AP4-induced JNK1 and miR-22-3p/FOSL1 feed-forward loop. AP4 binds to the E-boxes in *MAP3K13* and *FOSL1*. *MAP3K13* activates the JNK1 pathway, leading to AP-1 activation. *FOSL1* also activates AP-1. AP-1 promotes EMT, migration, invasion, and metastasis. miR-22-3p inhibits FOSL1.

often FOSL1-positive [6], and *MAP3K13* is up-regulated in colon cancer tissues [7]. Thus, AP4-induced *FOSL1* and *MAP3K13* are presumably clinically relevant in CRC. *FOSL1* showed a trend towards a positive correlation with AP4 in 471 primary CRC samples of The Cancer Genome Atlas Colon Adenocarcinoma (TCGA-COAD) cohort and in an independent patient cohort (GSE13294) (Supplementary Figure S2D). The dimerization of FOSL1 and c-Jun proto-oncogene (JUN) results in the formation of AP-1 [8]. Consistently, AP-1 activity was induced by ectopic AP4 (Figure 1D, Supplementary Figure S2E). In addition, AP-1 activity was significantly lower in AP4-deficient DLD-1 cells (Supplementary Figure S2F). Taken together, these results show that AP4 activates JNK1 and AP-1 by directly inducing *MAP3K13* and *FOSL1*.

Next, we analyzed the relevance of JNK1 for AP4-induced EMT. The JNK1 inhibitor DB07268 partially abrogated the induction of vimentin (*VIM*) and the repression of *CDH1* by AP4 in CRC cell lines (Supplementary Figure S3A), indicating that AP4-mediated JNK1 activation contributes to the induction of *VIM* and the *CDH1* repression by AP4 [3]. In addition, DB07268 significantly suppressed AP4-induced migration and invasion (Figure 1E, Supplementary Figure S3B-C). Furthermore, DB07268 largely suppressed the AP4-induced proliferation of DLD-1 cells (Supplementary Figure S3D). Therefore, JNK1 activation mediates the induction of EMT, migration, invasion and proliferation by AP4.

We have previously shown that AP4 represses the tumor-suppressive miRNA miR-22-3p, which contributes

respectively. (D) The AP-1 activity was determined by a dual-luciferase assay in DLD-1/pRTR-AP4-VSV cell after treatment with DOX for 48 hours to induce AP4 expression combined with transfection of 3xAP-1pGL3 reporter vector. The activated AP-1 promotes the expression of luciferase encoded by the reporter. (E) Cell migration (upper panel) was detected by a wound-healing assay in DLD-1/pRTR-AP4-VSV cells treated with DOX (AP4 activation) for 48 hours and for the last 24 hours with DB07268 (20  $\mu$ mol/L, JNK1 inhibitor). Cell invasion (lower panel) was detected by a Boyden-chamber assay in DLD-1/pRTR-AP4-VSV cells treated with DOX (AP4 activation) for 48 hours and for the last 24 hours with DB07268 (20  $\mu$ mol/L, JNK1 inhibition) for 48 hours. (F) Scheme of the miR-22-3p seed, the seed-matching sequences and its targeted mutation in the 3'-UTR of the *FOSL1* mRNA. The seed and seed-matching sequences are highlighted in red. (G) The direct targeting of *FOSL1* by miR-22-3p was validated by a dual-luciferase assay conducted 48 hours after SW480 cells were transfected with miR-22-3p mimic and human *FOSL1* 3'-UTR reporter. The results were normalized to cells transfected with control mimic. (H) Western blot analysis of *FOSL1* in DLD-1/pRTR-AP4-VSV cells transfected with miR-22-3p mimic and/or treated with DOX to induce AP4 expression for 48 hours. (I) qPCR (left panel) and Western blot (right panel) analysis of *FOSL1* in DLD-1 cells with the indicated *MIR22* status. For qPCR analysis, the expression of *FOSL1* mRNA in *MIR22*-deficient DLD-1 cells was normalized to *FOSL1* expression in *MIR22*-proficient DLD-1 cells. For Western blot analysis,  $\beta$ -actin served as a loading control. (J) Dual-luciferase assay analysis of AP-1 activity in DLD-1 cells with the indicated *MIR22* status. (K) qPCR analysis of the *FOSL1* mRNA decay rate in *MIR22*-deficient DLD-1 cells and *FOSL1*  $\Delta$ SMS DLD-1 cells after treatment with 10  $\mu$ g/mL of Actinomycin D for the indicated durations to block gene transcription. The results were normalized to *FOSL1* expression level at the 0-hour time-point in each cell line. (L) Western blot analysis of *FOSL1* in DLD-1 cells or *FOSL1*  $\Delta$ SMS DLD-1 cells after transfection with miR-22-3p mimic for 48 hours. (M) DLD-1/pRTR-AP4-VSV cells harboring wild-type *FOSL1* or *FOSL1*  $\Delta$ SMS were treated with DOX for 0, 24, 48 and 72 hours. *FOSL1* protein was determined by Western blot analysis. *FOSL1* protein levels were normalized to  $\alpha$ -Tubulin and untreated controls (0 hour DOX) and are shown above the corresponding protein signal.  $\alpha$ -Tubulin served as a loading control. (N) Cell migration (Left panel) was detected by a wound-healing assay in DLD-1/pRTR-AP4-VSV cells transfected with *FOSL1* siRNAs or/and treated with DOX (AP4 activation) for 48 hours. Cell invasion (right panel) was detected by a Boyden-chamber assay in DLD-1/pRTR-AP4-VSV cells transfected with *FOSL1*-specific siRNAs or/and treated with DOX (AP4 activation) for 48 hours. (O) Formation of lung metastases by DLD-1 Luc2/pRTR-AP4-VSV cells, which were treated with DOX or/and transfected with *FOSL1*-specific siRNA pools for 48 hours, then injected into tail-veins of NOD/SCID mice. Representative images of luciferase signals at the indicated time points after xenografting are shown. (P) The quantification of the luciferase signals in (O) is shown by total photon flux. (Q) Quantification of H&E staining is shown by metastatic nodules in the lungs from the four groups of mice in Figure S6A. (R) Formation of lung metastases by injecting DLD-1 Luc2/pRTR-AP4-VSV cells into the tail veins of NOD/SCID mice. DLD-1 Luc2/pRTR-AP4-VSV cells were treated with DOX (AP4 activation) for 48 hours and for the last 24 hours with DB07268 (20  $\mu$ mol/L, JNK1 inhibitor) before the injection. Representative images of luciferase signals at the indicated time points after xenografting are shown in Figure S6C. The quantification is shown as total photon flux. (S) Quantification of H&E staining is shown as metastatic nodules in the lungs of indicated mice in Figure S6C. (T) AP4, miR-22-3p and *FOSL1* form a coherent, regulatory feed-forward loop to activate *FOSL1*. In parallel, AP4 activates the JNK1 pathway. *FOSL1* and JNK1 activation leads to AP-1 activation, which ultimately induces EMT and metastases in CRC. In panels (A), (C-E), (G), (I-K), (N) and (Q-S), mean  $\pm$  SD ( $n = 3$ ) are shown. \*  $P < 0.05$ , \*\*  $P < 0.01$ , \*\*\*  $P < 0.001$ . Abbreviations: AP4: transcription factor AP4; MYC: c-MYC proto-oncogene; MAP3K13: mitogen-activated protein kinase kinase kinase 13; MAP2K7: mitogen-activated protein kinase kinase 7; JNK1: c-Jun N-terminal kinases 1; p-JNK1: phosphorylated c-Jun N-terminal kinases 1; FOSL1: Fos-like 1; AP-1: activator protein-1; GAPDH: glyceraldehyde 3-phosphate dehydrogenase; SNAIL: snail family transcriptional repressor 1; DOX: doxycycline; qPCR: quantitative polymerase chain reaction; ChIP: chromatin immunoprecipitation; 3'-UTR: 3'-untranslated regions;  $\Delta$ SMS: seed-matching sequence deletion; NOD/SCID: non-obese diabetic/severe combined immunodeficiency; H&E: hematoxylin and eosin; CRC: colorectal cancer; WT: wild-type; KO: knockout; MUT: mutant; gRNA: guide RNA; ns: not significant;  $t_{1/2}$ : time of half life; EMT: epithelial-mesenchymal transition; DMSO: dimethyl sulfoxide; Luc2: firefly luciferase 2; kD: kilodalton.



to the up-regulation of *mediator of DNA damage checkpoint 1* (*MDC1*), a miR-22-3p target, by AP4 [9]. Since we identified a miR-22-3p seed-match sequence (SMS) in the *FOSL1* 3'-untranslated region (3'-UTR), we investigated whether *FOSL1* is also regulated by AP4 via repression of miR-22-3p (Figure 1F). Indeed, a *FOSL1* 3'-UTR reporter was repressed by ectopic miR-22-3p, and mutation of the SMS rendered the reporter refractory to miR-22-3p (Figure 1G). Ectopic miR-22-3p repressed *FOSL1* (Supplementary Figure S4A) and effectively decreased basal and AP4-induced *FOSL1* protein levels (Figure 1H, Supplementary Figure S4B). Next, we generated *MIR22*<sup>-/-</sup> (*MIR22*-knockout [KO]) and *FOSL1*  $\Delta$ SMS CRC cell lines (Supplementary Figure S4C). *FOSL1* mRNA and protein expression were elevated in *MIR22*-deficient CRC cells (Figure 1I, Supplementary Figure S4D). *MIR22*-deficiency increased the activity of the *FOSL1* 3'-UTR reporter in a miR-22-3p SMS-dependent manner (Supplementary Figure S4E) and enhanced migration and invasion (Supplementary Figure S4F). Furthermore, the intrinsic AP-1 activity was significantly higher in *MIR22*-deficient CRC cells (Figure 1J, Supplementary Figure S4G). The half-life ( $t_{1/2}$ ) of *FOSL1* mRNA was prolonged in *MIR22*-deficient and *FOSL1*  $\Delta$ SMS DLD-1 cells (Figure 1K). Ectopic expression of miR-22-3p failed to repress *FOSL1* in *FOSL1*  $\Delta$ SMS CRC cells (Figure 1L, Supplementary Figure S4H), which showed increased basal *FOSL1* expression, and attenuated the up-regulation of *FOSL1* by AP4 (Figure 1M). Therefore, the direct targeting of *FOSL1* by miR-22-3p is essential for maintaining low levels of *FOSL1* expression, which allows *FOSL1* to be induced by AP4 directly and indirectly via repression of *MIR22*.

Next, we determined whether *FOSL1* mediates functional effects of AP4 on CRC cells. Ectopic AP4 repressed *CDH1* and induced *VIM* in CRC cells, and silencing *FOSL1* partially compromised these effects (Supplementary Figure S5A). The positive effect of ectopic AP4 on migration and invasion was largely abrogated by *FOSL1* silencing (Figure 1N, Supplementary Figure S5B-C), indicating that *FOSL1* mediates these effects of AP4. Silencing *FOSL1* significantly repressed AP-1 activity and compromised the effects of AP4 on AP-1 activity (Supplementary Figure S5D). In addition, ectopic AP4 induced the proliferation of DLD-1 cells, which was repressed by concomitant siRNA-mediated silencing of *FOSL1* (Supplementary Figure S5E). Taken together, these results demonstrate that the *FOSL1*-mediated activation of AP-1 by AP4 is required for the effects of AP4 on EMT, migration, invasion and proliferation.

miR-22-3p was shown to be significantly down-regulated in primary CRCs, which displayed lymph node metastasis, and ectopic miR-22-3p repressed lung metastasis formation in a xenograft model [10]. Therefore, deregulation of the miR-22-3p/*FOSL1* axis by AP4 may

be clinically relevant for mCRC. Notably, AP4 activation in non-metastatic DLD-1 cells allowed these to form lung metastases in non-obese diabetic/severe combined immunodeficiency (NOD/SCID) mice as determined by non-invasive bioluminescence imaging (Figure 1O-P) and histological analysis (Supplementary Figure S6A, right). Therefore, AP4 activation is sufficient to convert CRC cells from a non-metastatic to a metastatic state. Silencing *FOSL1* efficiently prevented the AP4-induced formation of lung metastases (Figure 1Q, Supplementary Figure S6A left). Therefore, *FOSL1* mediates and is required for the formation of AP4-induced metastases. Similar results were obtained after the inhibition of JNK1 using DB07268 (Figure 1R-S, Supplementary Figure S6B-C).

In conclusion, AP4 activates JNK1 and induces *FOSL1* directly, as well as indirectly, via repression of miR-22-3p. AP4, miR-22-3p and *FOSL1* form a coherent, regulatory feed-forward loop. These regulations converge in the activation of AP-1 (Figure 1T), which ultimately promotes EMT, migration and invasion, thereby enhancing metastasis formation. In the future, these findings may be exploited for the prevention and/or treatment of mCRC.

## DECLARATIONS

### AUTHOR CONTRIBUTIONS

Heiko Hermeking conceived, planned and supervised the project; Heiko Hermeking, Jinjiang Chou and Markus Kaller designed experiments; Jinjiang Chou performed experiments and analyzed results; Markus Kaller performed bioinformatics analysis; Matjaz Rokavec performed and analyzed mouse experiments. Fangteng Liu histochemically evaluated lung metastases in mice. Heiko Hermeking, Jinjiang Chou and Markus Kaller wrote the manuscript. All authors read and approved the final manuscript.

### ACKNOWLEDGMENTS

We are grateful to Raffaele Conca (Dr. von Haunersches Children's Hospital, Munich) for fluorescence-activated cell sorting and to Chunfeng Liu and Ursula Götz for technical assistance.

### CONFLICT OF INTEREST STATEMENT

The authors declare that they have no competing interests.

### CONSENT FOR PUBLICATION

Not applicable.

### FUNDING INFORMATION


This work was supported by German Cancer Aid/Deutsche Krebshilfe grants (70114235 and 70112245) to Heiko Hermeking.

## ETHICS APPROVAL

Animal experimentations and analyses were approved by the Government of Upper Bavaria, Germany (55.2-2532.vet\_02-18-57).

## DATA AVAILABILITY STATEMENT

All data generated or analyzed during this study are included in this article and its supplementary information files.

Jinjiang Chou<sup>1</sup>  
Markus Kaller<sup>1</sup>  
Matjaz Rokavec<sup>1</sup>  
Fangteng Liu<sup>1</sup>  
Heiko Hermeking<sup>1,2,3</sup> 

<sup>1</sup>*Experimental and Molecular Pathology, Institute of Pathology, Medical Faculty, Ludwig-Maximilians-Universität München, Munich, Germany*


<sup>2</sup>*German Cancer Consortium (DKTK), Partner site, Munich, Germany*

<sup>3</sup>*German Cancer Research Center (DKFZ), Heidelberg, Germany*

## Correspondence

Heiko Hermeking, Experimental and Molecular Pathology, Institute of Pathology, LMU Munich, Thalkirchner Strasse 36, Munich D-80337, Germany.  
Email: [heiko.hermeking@med.uni-muenchen.de](mailto:heiko.hermeking@med.uni-muenchen.de)

## ORCID

Heiko Hermeking  <https://orcid.org/0000-0001-6586-4406>

## REFERENCES

1. Siegel RL, Miller KD, Fuchs HE, Jemal A. Cancer statistics, 2022. *CA Cancer J Clin.* 2022;72(1):7-33.
2. Brabletz T, Kalluri R, Nieto MA, Weinberg RA. EMT in cancer. *Nat Rev Cancer.* 2018;18(2):128-134.
3. Jackstadt R, Roh S, Neumann J, Jung P, Hoffmann R, Horst D, et al. AP4 is a mediator of epithelial-mesenchymal transition and metastasis in colorectal cancer. *J Exp Med.* 2013;210(7):1331-1350.
4. Jung P, Menssen A, Mayr D, Hermeking H. AP4 encodes a c-MYC-inducible repressor of p21. *Proc Natl Acad Sci U S A.* 2008;105(39):15046-15051.
5. Fang JY, Richardson BC. The MAPK signalling pathways and colorectal cancer. *Lancet Oncol.* 2005;6(5):322-327.
6. Schmidt EM, Lamprecht S, Blaj C, Schaaf C, Krebs S, Blum H, et al. Targeting tumor cell plasticity by combined inhibition of NOTCH and MAPK signaling in colon cancer. *J Exp Med.* 2018;215(6):1693-1708.
7. Fu D, Ren Y, Wang C, Yu L, Yu R. LINC01287 facilitates proliferation, migration, invasion and EMT of colon cancer cells via miR-4500/MAP3K13 pathway. *BMC Cancer.* 2021;21(1):782.
8. Derijard B, Hibi M, Wu IH, Barrett T, Su B, Deng T, et al. JNK1: a protein kinase stimulated by UV light and Ha-Ras that binds and phosphorylates the c-Jun activation domain. *Cell.* 1994;76(6):1025-1037.
9. Chou J, Kaller M, Jaeckel S, Rokavec M, Hermeking H. AP4 suppresses DNA damage, chromosomal instability and senescence via inducing MDC1/Mediator of DNA damage Checkpoint 1 and repressing MIR22HG/miR-22-3p. *Mol Cancer.* 2022;21(1):120.
10. Xia SS, Zhang GJ, Liu ZL, Tian HP, He Y, Meng CY, et al. MicroRNA-22 suppresses the growth, migration and invasion of colorectal cancer cells through a Sp1 negative feedback loop. *Oncotarget.* 2017;8(22):36266-36278.

## SUPPORTING INFORMATION

Additional supporting information can be found online in the Supporting Information section at the end of this article.